Terahertz Biomedical Imaging: From Multivariate Analysis and Detection to Material Parameter Extraction

A. Al-Ibadi[1], **J. Bou Sleiman**[1], **Q. Cassar**[1], **G. Macgrogan**[2], **H. Balacey**[1], **T. Zimmer**[1], **P. Mounaix**[1], **and J. P. Guillet**[1]

[1]IMS, UMR CNRS 5218, Bordeaux University, France
[2]Institut Bergonié, Bordeaux, France

Abstract— Terahertz imaging is an interesting route for biomedical analysis. In particular, cancer imaging is a subject of study for different teams [1, 2]. A work is done in Bordeaux in partnership with a hospital to do terahertz analysis of breast tissue. This work is done in reflection with time domain imaging setup with fresh samples. The aim is to accurately assess tumor margins and which could in the future allow a quick validation of the precision of the surgical procedure and know if new surgery should be performed. We have presented in a previous paper [3] the use of automatic methods of image generation with different parameters [4] in order to explore the different contrasts that exist in the time and frequency domain data of a terahertz imaging system. These methods make it possible to locate and identify areas containing breast tissue, cancer or fat. In this communication, we propose to present new results and images with both multivariate approaches (like multivariate component analysis) and material parameter extraction to give both 2D localization and comprehensive parameter description.

1. INTRODUCTION

Many materials exhibit characteristic spectral features in the THz frequency range, directly related to their absorption line structures. The spectral features measured in THz spectra is generally attributed to intermolecular vibrations, intramolecular torsions, or even crystal-lattice vibrations. THz radiations probe collective motion of atoms, and through the excitation of intramolecular and intermolecular vibrations modes, it has the potential to provide both chemical and structural information

The techniques, used in medical imaging field such as X-ray, Magnetic Resonance Imaging (MRI) and fluorescence imaging, have several problem to detect the exact tumor margin during surgery [1]. These techniques are time consuming and too expensive. Moreover, imaging needs a dye injection into the body to determine the disease region.

In THz domain, many studies which have started to work on cancer detection, have found differences in tissues properties. The absorption coefficient and refractive index of fatty tissues are lower than cancer tissues, since fatty tissues have hydrocarbon chains and relatively few polar molecules [2]. However, the biological scattering is weak at THz wavelengths due to the interaction with only matter molecules became electronically excited. Thus, THz waves can provide a better contrast for soft tissues than other techniques [3].

Cancers will be visualized by imaging tools such as THz spectro-imaging. When THz beam with 1 THz and 4.14 meV passes through tissue, the reflected THz beam has information about optical properties of tissue under test and analysis these properties can be detected malignant and nonmalignant disease of tissue by THz spectral-imaging [2]. THz radiation, with low energy and absorption by high concentration in tissues which can penetrate and reach tissue depth, is sufficient to give information for diagnosis of tissue diseases [4].

Our goal in this study is to develop nondestructive and noncontact measurements such as terahertz spectral-imaging techniques for medical applications more precisely for breast cancer region in order to distinguish different parts of samples: fibro and adipose tissues. Furthermore, we wanted to obtain THz images of fresh and paraffin embedded breast tumor and compare it with corresponding visible imaged to show the differences among varied regions of the tissue. Terahertz images are obtained with automatic methods such as entropy.

2. MATERIALS AND METHOD

2.1. Sample preparation

Study samples (breasts with cancer) were obtained from Bergonie hospital. After excision of tissue, the chemical fixatives were used to prepare tissue according to histopathological protocol to

maintain the structure of the tissue such as proteins DNA, RNA, and amino acid. The biological tissue has major contents of water around 75 to 80% [5]. This water is very resistance to freezing and the bound water is a very small fraction of the total water in tissue. This frozen and fixated section was used for histological examination of the study tissue. This way allows determining that tumor has been completely removed during the surgery. Biological tissue has little inherent contrast in microscopy examination. Therefore, staining way used the standard protocol to give inherent contrast to the tissue. The frozen tissue have been sliced using a microtome into 3 to 5 µm mounted on glass slide and stained for histological observation of thin tissue under microscope to identify the cancerous and healthy tissue. Two types of tissues were prepared:

2.1.1. Paraffin Embedding of the Tissue

The breast tissue-paraffin was sliced with microtome into different thickness sections and mounted on transparency material for THz spectroscopy imaging study. The purpose of this preparation was to remove water from tissue and immerse into paraffin medium then solidified to allow sections to be cut as well as to recover structure of tissue from decade after fixation.

In this study, we focused on the ability of THz image contrast to investigate variation regions of the sample. The THz radiation can penetrate through several millimeters of the tissue. The sample was imaged in reflection mode of both Time Domain and Frequency Domain for comparing and monitor the changes occur in the measurements.

2.1.2. Fresh Tissue

Human fresh breast tissue was used in this study. After excision, tissue was submerged in NaCl which sustained tissue for a limited period until the time of THz imaging. The tissues were cut into sections by a microtome. The slices had no equal thickness and uneven surface.

2.2. Measurement System

Over the past decades, terahertz technologies are developed and several commercial systems are available in different configurations. In our case, portable and easy manipulated terahertz systems are needed for measurements inside surgery.

Terahertz time-domain spectroscopy (THz-TDS) is a broadband spectroscopic technique based on the use of ultrashort optical pulses to generate and detect a THz coherent pulse. By this method, both amplitude and phase of the THz electric field are measured. This allows direct determination of both the real and imaginary parts of the refractive index without having to resort to Kramers-Kronig relations.

In our study, we use two TDS systems from Teraview, the TPS3000 and TPS4000. The measurement was established on the TPS3000, but the advantage of the TPS4000 is the portability of the system, thus it can be used in the surgery [8].

(a) (b)

Figure 1. Photography of (a) Teraview TPS 3000 system and (b) TPS 4000 system. The TPS 4000 system is more compact and transportable.

Both systems offers a useful frequency range 0.2–3 THz with a maximum dynamic range around 75 dB, a spectral resolution of 0.06 THz and a rapid scan mode at the rate of 30 scans/second Air was used to keep the humidity in the THz chamber, all measurement were made at room temperature closed to 22 to 23°C. The spectral imaging is achieved by moving (X, Y) translating stage in the plane of the sample, thus we do a raster scanning with a maximum area of $16 \times 16\,\mathrm{mm}^2$ and gives access to spectral images in the focal plane (X, Y) after signal conversion from the temporal to the frequency domain.

Fresh tissue was removed from the NaCl prior the measurement. Thus fresh tissue slices were mounted between two quartz windows, each window was 3 mm in thickness. The problem of the tissue is difficult contact with quartz window because of the uneven surface of fresh tissue. The sample was exposure to THz beam by the raster scanning of the sample in the x-y plane. The tissue

was aligned with two window before scanning, a 2D image of the sample was generated where each pixel was recorded THz signal. The acquisition time from 5 to 13 hours of THz image dependent on the scan area of sample and step size of raster scan was 0.1 and 0.5 mm. The raw data was obtained by the time domain, and frequency domain.

Paraffin embedded tissue are measured with TPS 3000 system in reflection mode was used in this study. Tissue-paraffin embedded with 30 µm thickness was mounted on glass slide and silica window. The sample was exposure to THz beam by the raster scanning of the sample in the x-y plane. The tissue was aligned with window before scanning, a 2D image of the sample was generated where each pixel is recorded THz signal. The acquisition time from 1 to 1 : 15 hour of THz image dependent on the scan area of sample and step size of raster scan was 0.5 mm. The raw data was obtained by the time domain and frequency domain. The measurements were made in the 0.1–3.0 THz frequency.

3. SPECTRO-IMAGING RESULTS

3.1. Sample 1 Paraffin Embedded, a Mounted on Silica

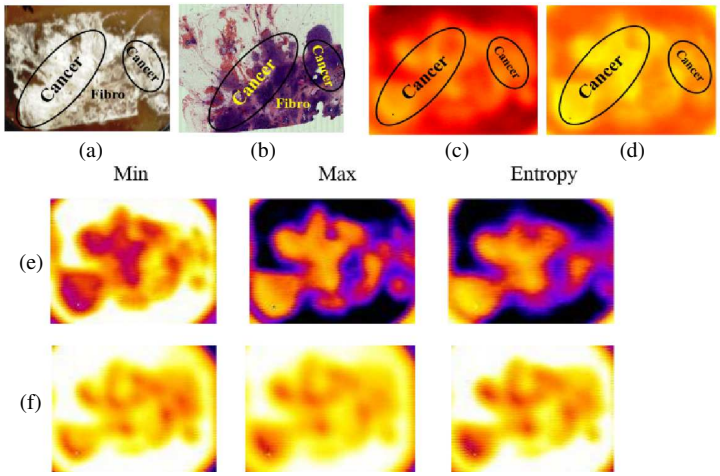

Figure 2. (a) visible image of tissue-paraffin embedded, (b) visible image of stain tissue used for correlation, THz images of raw data-reflection for 30 µm thickness of tissue as: (c) time domain image, (d) frequency domain image at 0.7 THz, Noctolyo analysis and vi.

3.2. Sample 2 (30 µm)-paraffin Embedded, a Mounted on Glass Slide

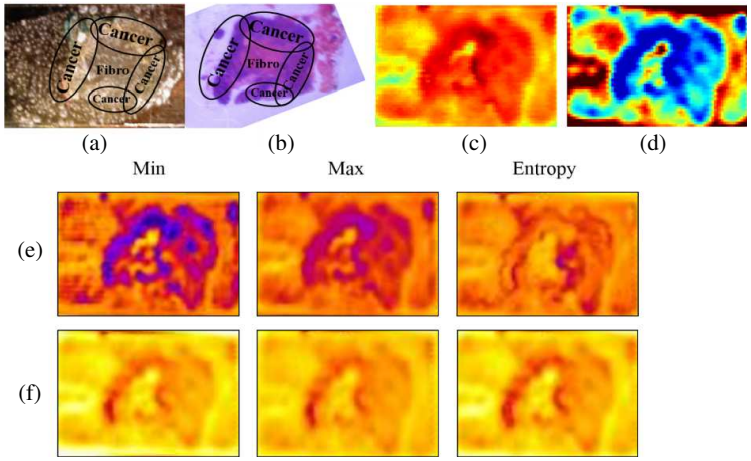

Figure 3. (a) visible image of tissue-paraffin embedded, (b) visible image of stain tissue used for correlation, THz images of raw data-reflection for 30 µm thickness of tissue as: (c) time domain image, (d) frequency domain image at 0.9 THz, Noctolyo analysis and visualization of raw data-reflection as: (e) Min, Max, and Entropy at time domain, (f) Min, Max, and Entropy at frequency domain.

3.3. Sample 3, fresh tissue

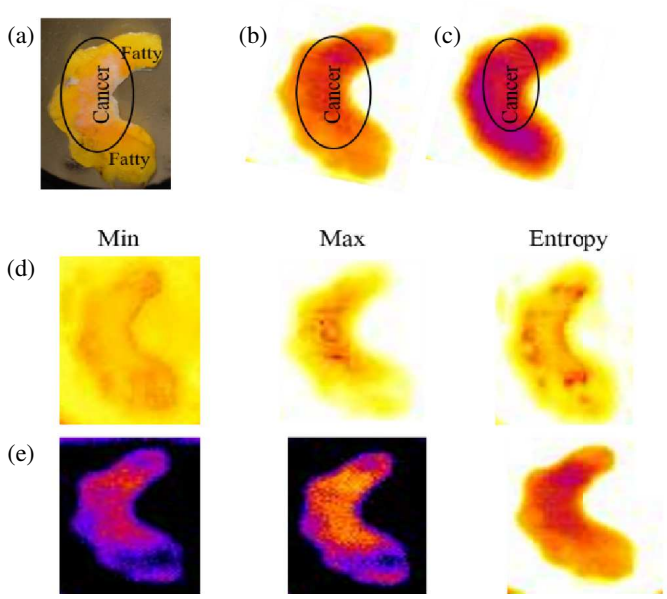

Figure 4. (a) visible image of fresh breast tissue. THz images of raw data-reflection for fresh tissue as: (b) time domain image, (c) frequency domain image at 0.6 THz. Noctolyo analysis and visualization of raw data-reflection as: (d) Min, Max, and Entropy at time domain, (e) Min, Max, and Entropy at frequency domain.

3.4. Sample 4, fresh tissue

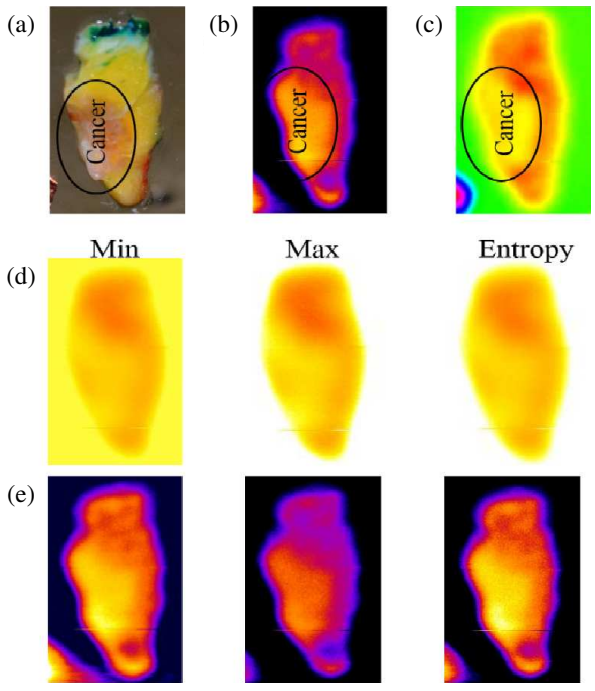

Figure 5. (a) visible image of fresh breast tissue. THz images of raw data-reflection for fresh tissue as: (b) time domain image, (c) frequency domain image at 0.4 THz. Noctolyo analysis and visualization of raw data-reflection as: (d) Min, Max, and Entropy at time domain, (e) Min, Max, and Entropy at frequency domain.

4. DISCUSSION

We first wanted to compare visible images of paraffin embedded breast tumor samples with THz images, to show the differences among varied regions of the tissue.

Figures 2(a) and 3(a) shows the visible image of tissue-paraffin embedded. The thickness of this tissue was 30 µm, and it was mounted on silica and glass slide window, respectively. We could identify the cancerous region that was more dense than other regions of the sample. Moreover, the coloration of the sample with eosin. Showed that the cancer tissue was darker (Figures 2(b) and 3(b)). This difference in coloration corresponds to an increased cell concentration due to the presence of cancer cells in the tissue containing nuclei and nucleoli, as well as the increased vascularization that is typical for tumor, to satisfy the increased need for oxygen due to the high metabolic rate of cancer cells. This result shows that the coloration of regions corresponds to the type the region of the tissue such as cancer, fibro, and fatty.

On the other hand, Figures 2(c), (d) and 3(c), (d) shows the THz images of raw data that was obtained from THz spectroscopy in reflection mode at 14 ps, 10 ps in time delay respectively, and 0.7 THz, 0.9 THz in frequency domain, respectively. The raw data, formed from Min, Max, and entropy in time domain and frequency domain, respectively Figures 2(e), (f), and 3(e), (f). We obtained detailed 2D imaging in areas of tissues where variations in the concentrations and contrast of different regions of these samples were observed.

We also performed histopathologic diagnosis on two fresh samples (Figure 4(a) and Figure 5(a). We found that samples was formed of two inhomogeneous regions: the cancerous tissue that was more thick, than the normal tissue. Figures 4, 5(b) and (c): shows the images of raw data corresponding of the THz spectroscopy in reflection mode at 27 ps, 6 ps in time delay respectively, and 0.6 THz, 0.4 THz in frequency domain, respectively. Moreover, the raw data was formed from Min, Max, and entropy in time domain and frequency domain, respectively, as shown in (Figures 4(d), (e) and 5(d), (e). We obtained detailed 2D imaging in areas of tissues where variations in the concentrations and contrast of different regions of these samples were observed.

We used noctylab software solution of imaging which was applied to all THz images to extract and analyze information about the samples. THz images show the high concentrations and high contrast at cancer region compared to other regions of tissue, indicating that the water was content in the tumor breast tissue. Clearly, the THz images allow differentiating between different regions of tissue. The information in the THz images is similar to that observed in the visible image of similar tissue areas.

Numerous groups worked with THz imaging of fresh tissues, tissues fixed with formalin and tissues embedded in paraffin prior to the experiments. They were able to identify contrast between cancer affected tissues and the adjacent normal tissue. They also found that the contrast was higher in freshly excised tissue [6]. Another research was done by S. Joseph et al. to identify different types of cancers, and they found that water has a good effect on contrast cancer diagnosis [7].

Figure 7 shows the visible image again of tissue with the selected points and the frequency-dependent refractive index and absorption coefficient were extracted from raw data reflected of the fresh tissue (tumor and normal regions) and water using the reflection terahertz spectroscopy system From the plots, differences between all tissue regions and water are consistent over frequency rang. Figure 7(a) illustrate the results of the refractive index for all tissue regions and water. The refractive index of the tumor is higher than in normal tissue, and it was compared with the refractive index of water. In all cases, the refractive index decreases with frequency. Figure 7(b) illustrate the results of the absorption coefficient for all tissue regions and water. The absorption coefficient of tumor is higher than normal tissue were compared with the absorption coefficient of water. In all cases, the absorption coefficient increases with frequency.

As a result, the optical properties of the sample were calculated using baseline method with terahertz frequencies in reflection mode.

4.1. Parameter Extraction on One Pixel

4.1.1. Method

The data was recorded on a 4000 Tera Pulse system in reflection mode by a detector and Fourier transformed through a numerical operation. Reflection signals were collected from the air-quartz surface to be used as a reference signal, and signals were collected from the quartz-water. In this study, the quartz was used with window (window/quartz) for measuring the reflection THz pulse as a baseline. Signals were collected from the quartz-water, and quartz-samples. All reflection measurements were recorded at 10 deg of incident angle. A 100 ps measurement window had 4096

data points collected with a sampling interval of 0.008 ps. As shown in Figure 6. Absorption and refractive index extraction shows fluctuation between bad tissue and normal tissue (see Figure 7).

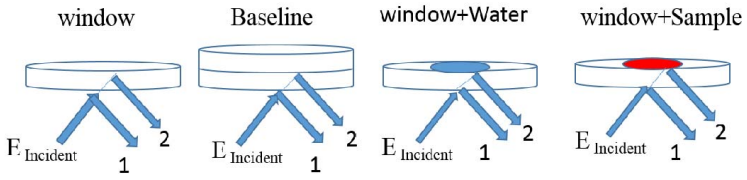

Figure 6. Schematic diagram of four measurement in reflection geometry for reference, baseline, water, and sample.

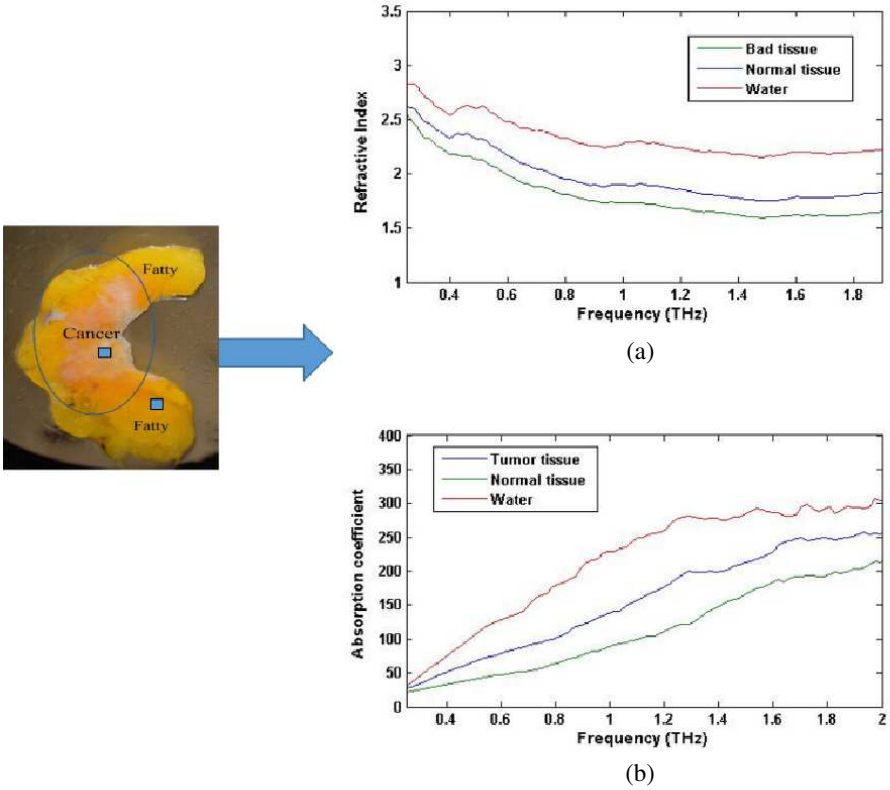

Figure 7. The terahertz properties for water and breast tissue. (a) Refractive index and (b) Absorption coefficient calculated of tumor (blue line), normal region (green line), and water (red line).

5. CONCLUSION

We measured several paraffin embedded and fresh tissues breast cancer samples with the reflection terahertz spectroscopy imaging system. From the profile data measured at each pixel, the time domain and frequency domain images we found contrast between the tumor region and the normal region. By THz images processes by noctilyo, we could determine the cancer tissue distribution, it is needed to compare THz images and histopathologic diagnosis for various regions sample.

A reflection THz pulsed spectroscopy system was used to study the interaction of THz pulses with for breast cancer, through analysis of the sample properties in the frequency bandwidth of both refractive index and absorption coefficient Absorption and refractive index fluctuation between bood and bad tissues could be used in the future to develop a model allowing to detect and identify bad tissue quickly.

REFERENCES

1. Oh, S. J., S.-H. Kim, Y. Bin Ji, K. Jeong, Y. Park, J. Yang, D. W. Park, S. K. Noh, S.-G. Kang, Y.-M. Huh, J.-H. Son, and J.-S. Suh, "Study of freshly excised brain tissues using terahertz imaging," *Biomed. Opt. Express*, Vol. 5, No. 8, 2837–2842, 2014.
2. Yu, C., S. Fan, Y. Sun, and E. Pickwell-Macpherson, "The potential of terahertz imaging for cancer diagnosis: A review of investigations to date," *Quantitative Imaging in Medicine and Surgery*, Vol. 2, 33–45, 2012.
3. Wilmink, G. J. and J. E. Grundt, "Invited review article: Current state of research on biological effects of terahertz radiation," *J. Infrared, Millimeter, Terahertz Waves*, Vol. 32, 1074–1122, 2011.
4. Zaytsev, K. I., K. G. Kudrin, S. A Koroleva, I. N. Fokina, S. I. Volodarskaya, E. V Novitskaya, A. N. Perov, V. E. Karasik, and S. O. Yurchenko, "Medical diagnostics using terahertz pulsed spectroscopy," *J. Phys. Conf. Ser.*, Vol. 486, 012014, 2014.
5. Huff-Lonergan, E. and S. M. Lonergan, "Mechanisms of water-holding capacity of meat: The role of postmortem biochemical and structural changes," *Meat Sci.*, Vol. 71, 194–204, 2005.
6. Fitzgerald, A. J., et al., "Terahertz pulsed imaging of human breast tumors," *Radiology*, Vol. 239, 533–540, 2006.
7. Joseph, C. S., A. N. Yaroslavsky, M. Al-arashi, T. M. Goyette, C. Jason, A. J. Gatesman, B. W. Soper, C. M. Forgione, T. M. Horgan, E. J. Ehasz, R. H. Giles, and W. E. Nixon, "Terahertz spectroscopy of intrinsic biomarkers for non-melanoma skin cancer," *SPIE 7215, Terahertz Technol. Appl. II*, 72150I, 2009.
8. Balacey, H., A. Al-Ibadi, G. Macgrogan, J. P. Guillet, E. MacPherson, and P. Mounaix, "Automated data and image processing for biomedical sample analysis," *2016 41st International Conference on Infrared, Millimeter, and Terahertz waves (IRMMW-THz)*, 1–2, Copenhagen, 2016, doi: 10.1109/IRMMW-THz.2016.7758882.